IEEE Access
Multidisciplinary | Rapid Review | Open Access Journal

Received December 10, 2019, accepted December 17, 2019, date of publication December 20, 2019,
date of current version January 3, 2020.

Digital Object Identifier 10.1109/ACCESS.2019.2961246

Quadcopter Control System Using a Hybrid BCI Based on Off-Line Optimization and Enhanced Human-Machine Interaction

NONG YAN[1,2,3,4], CHANG WANG[1], YI TAO[1,2,3,4], JINMING LI[1], KEXU ZHANG[1], TING CHEN[1], ZIWEN YUAN[5], XIANGGUO YAN[1,2,3,4], AND GANG WANG[1,2,3,4], (Member, IEEE)

[1]The Key Laboratory of Biomedical Information Engineering of Ministry of Education, School of Life Science and Technology, Institute of Biomedical Engineering, Xi'an Jiaotong University, Xi'an 710049, China
[2]National Engineering Research Center for Healthcare Devices, Guangzhou 510500, China
[3]The Key Laboratory of Neuro-informatics and Rehabilitation Engineering of Ministry of Civil Affairs, Xi'an Jiaotong University, Xi'an 710049, China
[4]Guangdong Provincial Key Lab of Medical Electronic Instruments and Polymer Material Products, Guangdong Institute of Medical Instruments, Guangzhou 510500, China
[5]Department of Rehabilitation, First Affiliated Hospital, Xi'an Jiaotong University, Xi'an 710061, China

Corresponding author: Gang Wang (ggwang@xjtu.edu.cn)

This work was supported in part by the National Natural Science Foundation of China under Grant 31571000, Grant 61471291, Grant 61431012, and Grant 81201162, in part by the Natural Science Basic Research Plan in Shaanxi Province of China under Grant 2013JQ8007, in part by the Fundamental Research Funds for the Central Universities of China under Grant xjj2017122, and in part by the Science and Technology Planning Project of Guangdong Province under Grant 2017B030314174.

ABSTRACT Quadcopter is an important way for the human to explore the physical world. The brain-computer interface (BCI) technology is used to control the quadcopter flight in order to help disabled persons communicate with the external world freely. In this study, a quadcopter control system using a hybrid BCI based on off-line optimization and enhanced human-machine interaction was designed to control the quadcopter flight in 3D physical space. The proposed system implemented the control of quadcopter moving up/down, forward/backward, left/right by six different SSVEP, and turning left/right by left-hand and right-hand motor imagery. Meanwhile, the optimization of the control system and the human-machine interaction enhancement improved practicability in real-time use. Five subjects participated in an on-line experiment to control the quadcopter flight in real-time. The average classification accuracy of EEG-based commands in the on-line experiment was 87.09±2.82% and information transfer rate (ITR) was 0.857±0.085 bits/min. The results demonstrated the feasibility of multidirectional control of quadcopter flight in 3D space by using hybrid BCI technology and revealed the practicality and operability of the hybrid BCI control system based on off-line optimization and human-machine interaction enhancement.

INDEX TERMS Quadcopter control system, motor imagery, steady-state visual evoked potential, off-line optimization, human-machine interaction.

I. INTRODUCTION

In recent years, the brain-computer interface (BCI), as technology in connecting the human brain with the external world, has been widely concerned due to the increasing needs and fast development of the human-machine interface. The BCI is aimed at assisting persons with severe motor function disability to communicate with the external world freely [1]. Meanwhile, the BCI has been applied to human-computer interaction, virtual reality and human-robot coordination [2]–[4]. The quadcopter, as an important way for the human to explore the physical world, becomes an emerging application in human daily life, which has the advantage of multi-degree of freedom(MDOF) and simple operation to meet the demands of multidirectional and continuous control. Therefore the BCI and quadcopter control can be combined to explore the external world directly with users' intention [5].

The quadcopter control system based on BCI is mainly divided into SSVEP-based BCI and motor imagery-based BCI. In the applications of SSVEP-based BCI, Lenis et al. proposed an asynchronous system, which accomplished the control of quadcopter in 3D space by six different frequencies visual stimuli, and the detection of the idle state was introduced in this control system to avoid the fatigue of users [6]. Meng et al. achieved the control of quadcopter

The associate editor coordinating the review of this manuscript and approving it for publication was Peng Xu.

flight using visual stimuli with four different frequencies by a head-mounted device where all stimuli and feedbacks were presented [7]. The flexible frequencies of visual stimuli generated by the sinusoidal modulation method can ensure a large number of commands in quadcopter control [8]. However, there is a weak correlation between SSVEP and users' intention, and the continuous visual stimuli will make users fatigue and discomfort [9]. In the applications of motor imagery-based BCI, Lafleur et al. controlled the vertical and rotated flight of quadcopter by motor imagery while the quadcopter went forward with a constant velocity [10]. Shi et al. constructed a semi-autonomous quadcopter system that was designed to select the feasible directions from the motor imagery-based navigation system to control the quadcopter flight [11]. The motor imagery-based BCI usually consists of left-hand, right-hand, feet, leg and tongue tasks [12], [13]. The limited number of imagery tasks will restrict the degree of freedom (DOF) in quadcopter control. However, the motor imagery-based BCI maintains a more direct correlation between EEG signals and users' intention than SSVEP-based BCI [14]. In addition, the hybrid BCI based on EEG, EMG, and EOG were also used in quadcopter control [15], [16]. Kim et al. accomplished the eight angles of quadcopter flight control by the combination of EEG signals and eye-tracking [17]. Khan et al. proposed a control system based on eight commands by using EEG signals and near-infrared spectral signals [18]. The hybrid BCI based on the multi-signals was similar to the SSVEP-based BCI which lacks the correlation between signals and users' intentions [19]. Some studies have demonstrated the feasibility of quadcopter control by combining SSVEP-based BCI and motor imagery-based BCI in the physical world. Duan et al implemented the quadcopter control using multi-modal BCI in the physical environment [20], [21]. However, this quadcopter control system would cause fatigue due to using the eye-blinking to distinguish SSVEP and motor imagery modalities. Besides that, lacking analysis of the off-line experiment could not offer optimal configurations to control system which may reduce the performance of the system in real-time.

To solve the challenges mentioned above, a quadcopter control system using a hybrid BCI based on off-line optimization and enhanced human-machine interaction was designed to control the quadcopter flight in 3D physical space. On one hand, off-line optimization was performed to choose the optimal number of channels and recorded data length used in on-line experiments. On the other hand, the human-machine interaction was enhanced by providing feedback information, switching of SSVEP and MI base on the eyes-closed state, and LCD-cued SSVEP and MI.

II. METHODS AND EXPERIMENTS

A. QUADCOPTER CONTROL SYSTEM BASED ON HYBRID BCI

In this study, the hybrid BCI technology was used to control the quadcopter flight with multiple commands in 3D physical space. The architecture of quadcopter control system based on the hybrid BCI is shown in Figure 1. Firstly, the users gazed at the visual stimulus corresponding to the intentional control command on the stimulator interface. The data acquisition device recorded the scalp EEG and sent it to the data processor. Then the scalp EEG data was processed by the data processor and translated into a control command. The position information of the quadcopter and the system control flag were updated according to the control command. After the android controller received the control command, the quadcopter was controlled via Wi-Fi. Meanwhile, the first-view images captured by the camera of quadcopter were sent back to the data processor. Finally, the feedback information contained first-view images and the quadcopter position information was shown on the visual feedback interface. The system control flag was sent to the stimulator interface to switch the sub-control interfaces.

1) STIMULATOR INTERFACE

The stimulator interface is shown in Figure 2. The sub-control interfaces of stimulators consisted of initialization interface, control interface with SSVEP-based visual stimulations and control interface with MI-based visual cues. The frequencies of visual stimuli were chosen from 8Hz to 14Hz, due to the high SNR of SSVEP signals [22]. The initialization interface was designed to control quadcopter taking off and landing. The frequencies of visual stimuli were 8, 10 and 12Hz, which indicated the commands of interface switching, quadcopter taking off and landing. The function of the control interface with SSVEP-based visual stimulations was providing visual stimuli for users to control the quadcopter straight flight. The frequencies of visual stimuli were 8Hz to 14Hz, which indicated quadcopter move up/down, forward/backward, left/right. The stimulator interface was presented on a 24.5-inch LCD screen with a refresh rate of 120Hz. The visual stimuli were generated by the sinusoidal stimulation method [8]. The stimulus program was developed on MATLAB using Psychophysics Toolbox [23]. The function of the control interface with MI-based visual cues was providing visual cues for users to control the rotated flight of quadcopter. Circling with a pen by hands was selected as visual cues to ensure the correlation between users' intention and quadcopter control, indicated the turning left and turning right of the quadcopter [14].

2) VISUAL FEEDBACK INTERFACE

The visual feedback interface is shown in Figure 3. The visual interface displayed the first-view images captured by the camera of quadcopter and the quadcopter position information in real-time. Meanwhile, the position of targets, the present position of quadcopter and the landing location showed on the interface. The feedback information helped users to find an appropriate control strategy and make right control commands in quadcopter flight, which enhanced the human-machine interaction of the control system. The visual feedback interface was presented on a 22-inch LCD screen and developed on MATLAB.

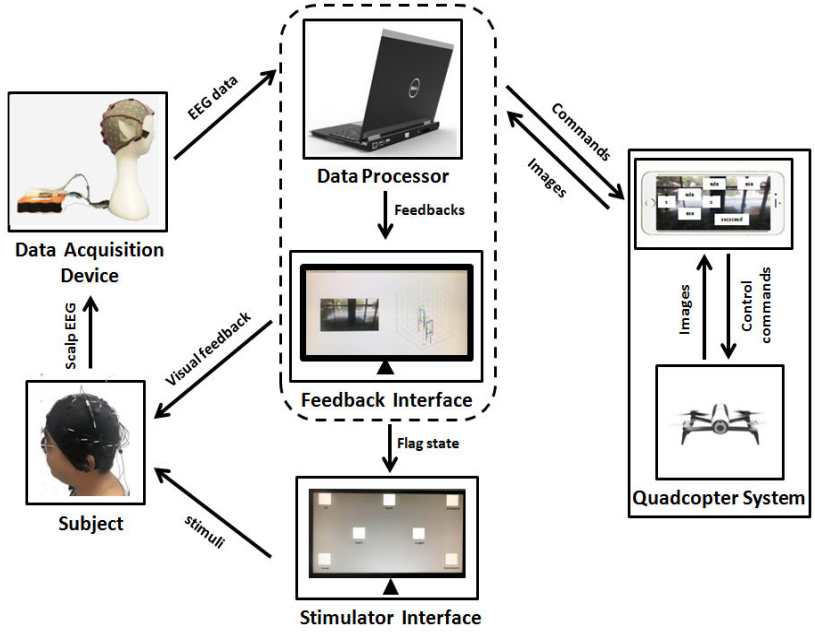

FIGURE 1. Architecture of quadcopter control system based on hybrid BCI. The system consists of data acquisition device, data processor, stimulator interface, visual feedback interface and quadcopter system. The arrow indicates the direction of the data stream. The dotted box shows that data processor and visual feedback interface share the same computer host.

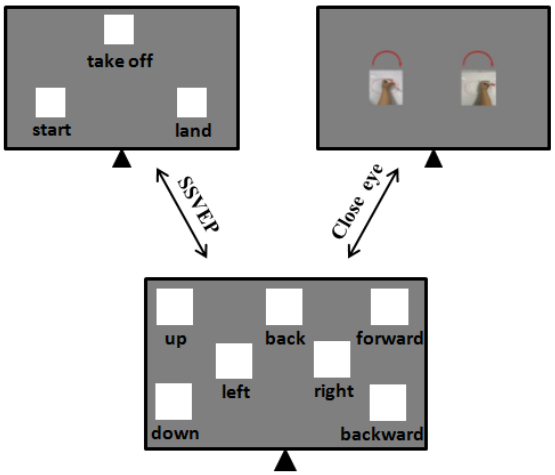

FIGURE 2. Stimulator interface. The stimulator interface consists of initialization interface, control interface with SSVEP-based visual stimulations and control interface with MI-based visual cues. The initialization interface and control interface with SSVEP-based visual stimulation are switched by SSVEP, shown as start and back cues on interface. The switch between control interface with SSVEP-based visual stimulations and control interface with MI-based visual cues are achieved by EEG in eyes close state.

3) DATA ACQUISITION DEVICE

The scalp EEG was recorded by using the 16-channels g.USBamp with a sampling rate of 256Hz. 14 electrodes were recorded (C1, C2, C3, C4, Cz, Pz, P3, P4, POz, PO3, PO4, Oz, O1, O2) on the visual cortex and sensorimotor cortex, according to the international 10-20 system. The reference electrode was selected at FPz, and the ground electrode was selected at the right mastoids. Electrode impedances were kept under 10 kΩ. To improve the SNR of scalp EEG, a 5-30Hz bandpass filter was applied in EEG recording [24].

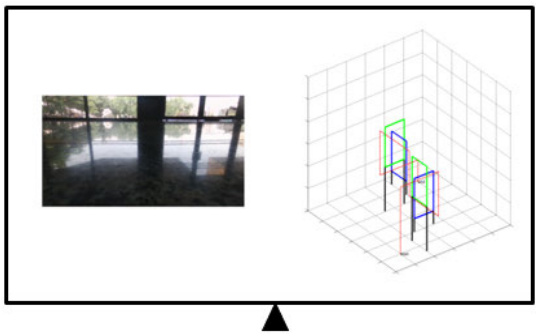

FIGURE 3. Visual feedback interface. On the left side was the images captured by the camera of quadcopter. On the right side was the position information of the quadcopter.

4) DATA PROCESSOR

The data processor was designed to process EEG from the data acquisition device. The processing steps contained preprocessing, feature extraction, classification, and signals translation. Meanwhile, the data processor updated the system control flag according to the translated command. The feedback information was sent to the visual feedback interface and the updated system control flag was sent to the stimulator interface. The updated system control flags based on control commands are shown in Table 1.

5) QUADCOPTER SYSTEM

The quadcopter used in the system is Parrot Bebop 2 due to the sustainable development and strong stabilization [6], [7], [10], [11], [17], [18]. In the proposed system, eight EEG-based control commands transmitted via the wireless network to control the quadcopter flight in 3D space.

TABLE 1. The updated system control flags based on the commands to switch the sub-control interface.

Command	Stimuli	Interface	System control flag	updated flag
Start	8Hz	Initialization Interface	0	1
Land	10Hz	Initialization Interface	0	0
Take off	12Hz	Initialization Interface	0	0
Up	8Hz	SSVEP-based Interface	1	1
Down	9 Hz	SSVEP-based Interface	1	1
Back	12 Hz	SSVEP-based Interface	1	0
Forward	10 Hz	SSVEP-based Interface	1	1
Backward	11 Hz	SSVEP-based Interface	1	1
Left	13 Hz	SSVEP-based Interface	1	1
Right	14 Hz	SSVEP-based Interface	1	1
Y-Left	left hand	MI-based Interface	2	2
Y-Right	Right hand	MI-based Interface	2	2
Close eyes	/	/	2/1	1/2

TABLE 2. The movement displacement and yaw angle of the control commands based on the control time.

Command	Movement	stimuli	Control time(ms)	Displacement/angle
Up	Move up	8Hz	800	1.2m
Down	Move down	9Hz	800	1.2m
Forward	Move forward	10Hz	2200	3.3m
Backward	Move backward	11Hz	2200	3.3m
Left	Move left	13Hz	1000	1.5m
Right	Move right	14Hz	1000	1.5m
T-Left	Turn left	left hand	7000	87.5°
T-Right	Turn right	right hand	7000	87.5°
Take off	Take off	12Hz	1100	1.65m
Land	Land	10Hz	——	——

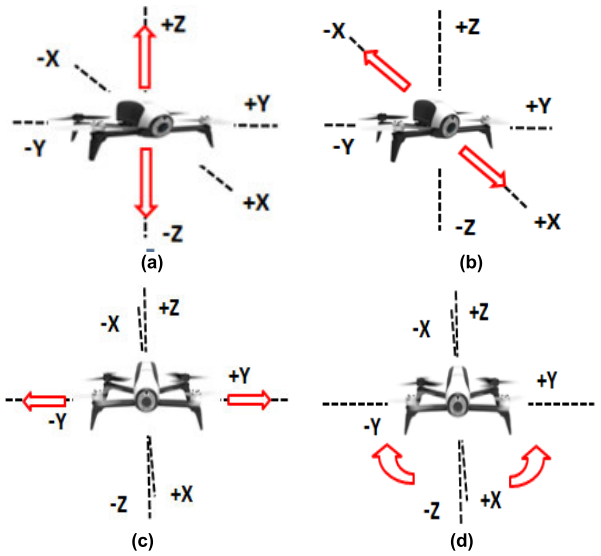

FIGURE 4. The control of quadcopter. (a) Move up/down in straight flight (b) move forward/backward in straight flight (c) move left/right in straight flight (d) turn left/right in rotated flight.

The control of the quadcopter is shown in Figure 4. The straight flight indicated quadcopter moving in the straight line, including moving up/down, moving forward/backward, moving left/right. The rotated flight indicated quadcopter turning left/right. The left/right movements of quadcopter were designed to adjust the quadcopter position to reduce the location errors caused by the low control precision of quadcopter. Meanwhile, the android controller based on the mobile app was designed to control the movement displacements and yaw angles in quadcopter flight. The quadcopter control times were adjusted to select the optimal displacement and angle when the speed of quadcopter is set at a constant. The straight movement speed of quadcopter is set at 1.5m/s, and the rotation speed of quadcopter is set as 12.5°/s. The movement displacements and yaw angles of control commands are shown in Table 2.

B. METHODS

In the proposed system, the scalp EEG filtered in 5-30Hz was recorded with 14 electrodes on the position of visual cortex and sensorimotor cortex, and translated into the control command to control the quadcopter flight. The most prominent challenge in the algorithm of the system is the classification of SSVEP and motor imagery [9], [25], [26]. the EEG in eyes-closed state was chosen as the switch signal of two modal EEGs. The detection of EEG in eyes-closed represented the switching from one modal to the other modal. This design could reduce the fatigue of users and increase the classification accuracy of two modals EEG, which ensure the practicability and operability of the control system. The classification of SSVEP was achieved by the canonical correlation analysis (CCA) algorithm, and the classification of motor imagery was achieved by the combination of common spatial pattern algorithm and linear distinction analysis algorithm. The classification results were translated into the control commands to control the quadcopter flight. The flow chart of the classification algorithm is illustrated in Figure 5.

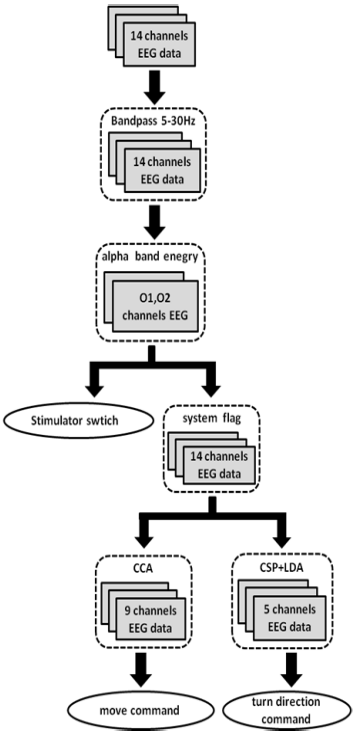

FIGURE 5. The flow chart of BCI algorithm in data processor. The data processing included the detection of eyes close and open, SSVEP classification and motor imagery classification.

1) DETECTION OF EYES CLOSED AND OPEN

The EEG in the eyes-closed and eyes-open state recorded on the position of the visual cortex was discriminated by the power in the alpha-band due to the alpha-band power obviously rose in the eyes-closed state [27]–[29]. X indicates the filtered EEG recorded with 3 electrodes (O1, O2, Oz) on the visual cortex [30]. The EEG was divided into several frequency bands EEG by wavelet packet decomposition [31]–[34]. The powers of divided EEG are calculated as the following (1). Y, E indicates the EEG in the alpha band and the power in the alpha band [35], [36]. The percentage φ of the alpha-band power in EEG signals was calculated as following (2), in which Y and X indicated the EEG in the alpha band and unfiltered EEG signals.

$$E = \sum YY^T \tag{1}$$

$$\varphi = \frac{\sum YY^T}{\sum XX^T} \tag{2}$$

The classification threshold was calculated by (3), in which φ_1, φ_2 were the alpha power percentage in the eyes-closed state and eyes open state. The detections of the eyes-closed state and the eyes-open state were depended on comparison results between the power percentage φ and the power threshold v in (4).

$$v = 4 \times \varphi_1 + 1 \times \varphi_2 \tag{3}$$

$$\left\{ \begin{array}{l} \varphi < v, K \in eyes\ close \\ \varphi > v, K \in eyes\ open \end{array} \right\} \tag{4}$$

2) SSVEP CLASSIFICATION

Canonical correlation analysis (CCA) was chosen as the algorithm of SSVEP classification for its high accuracy and robustness [37], [38]. The CCA algorithm constructed the template signals with the frequencies of visual stimuli, maximized the correlation coefficient between the template signals and SSVEP, and selected the frequency of template signals with the maximal correlation coefficient as the frequency of SSVEP [39].

X indicates the EEG recorded with 9 electrodes (Pz, P3, P4, POz, PO3, PO4, Oz, O1, O2) on the visual cortex [40]. Y indicates the sine and cosine signals with frequencies of visual stimuli, shown in (5). f_i indicates the frequency of visual stimuli [41].

$$Y = \begin{bmatrix} Y_1 \\ Y_2 \\ \cdots \\ Y_K \end{bmatrix} = \begin{bmatrix} \sin(2\pi f_1 t); \cos(2\pi f_1 t); \\ \sin(2\pi f_2 t); \cos(2\pi f_2 t); \\ \cdots \\ \sin(2\pi f_K t); \cos(2\pi f_K t); \end{bmatrix} \tag{5}$$

CCA provided the spatial filter a, b to maximize the Pearson correlation coefficient ρ_i between X and Y_i ($i = 1, ..K$) as the following (6). The frequency with the maximal correlation coefficient ρ_s between X and Y_i was selected as the frequency of SSVEP in (7) [42].

$$\rho_i = \frac{E(a^T X b_i^T Y_i)}{\sqrt{E(a^T X)E(b_i^T Y_i)}} \tag{6}$$

$$\rho_s = \max(\rho_i) \tag{7}$$

3) MOTOR IMAGERY CLASSIFICATION

The classification of motor imagery was implemented by combining the common spatial pattern algorithm and the linear distinction analysis algorithm. Firstly, the features were extracted from the motor imagery by the common spatial pattern algorithm. After that, motor imagery was classified by the features with the linear distinction analysis algorithm [43].

The motor imagery EEG was recorded with 5 electrodes (C1, C2, C3, C4, Cz) on the position of sensorimotor cortex. The training motor imagery EEG is divided into the left-hand dataset X_1 and the right-hand dataset X_2. The spatial filter W was calculated from the training dataset by CSP method. The feature extraction of EEG is shown in (8). Z_1, Z_2 indicated the feature series of left-hand dataset and right-hand dataset.

$$Z_1 = W^T X_1, \quad Z_2 = W^T X_2 \tag{8}$$

The linear classifier was constructed by feature series of two classes dataset in equation (9). m_1 , m_2 indicated the mean of two classes dataset. S_b, S_w indicated the intra-class and inter-class variance. W_b, b are the parameters of the linear classifier.

$$W_b = S_w^{-1}(m_1 - m_2), \quad b = -W_b(0.5m_1 + 0.5m_2) \tag{9}$$

The classification results of the test dataset T achieved by the linear classifier. p is the output of the linear classifier

calculated by the equation (10), When $p > 0$, the test dataset T belongs to the left-hand motor imagery. When $p < 0$, the test dataset T belongs to the right-hand motor imagery.

$$p = w_b^T T + b \tag{10}$$

C. EXPERIMENTAL PARADIGM

The performance of the control system was evaluated in two experiments, an off-line experiment I and an on-line experiment II. The experimental procedures were approved by Xi'an Jiaotong University Ethics Committee. The off-line experiment I was designed to test the accuracy and robustness of the algorithm in extracting features and classifying the control intentions from scalp EEG. Meanwhile, the results of the off-line experiment I gave support to the parameter selection of the control system. The on-line experiment II was designed to evaluate the BCI control capacity of the system, by controlling quadcopter going through targets and reaching the designated position. All subjects were recruited from Xi'an Jiaotong University. They were informed of the purpose and procedure of experiment I and experiment II, and signed informed consents before the experiment.

Ten subjects (5 males, 5 females), at the age of 20 to 24 (averaged age 22.7), participated in the off-line experiment I. All participants have no history of epilepsy, and normal or corrected to normal eyesight. During the off-line experiment procedure, subjects sat with a distance of 70 cm between the monitor and their eyes, and kept no movement with the body as possible as they can. Meanwhile, the environmental factors, such as lighting, were maintained at a comfortable level for subjects to help them keep sober and focused. Off-line experiment I contained 3 sessions, including SSVEP session 1, motor imagery session 2 and eyes-closed session 3. Each trial in session 1 and session 2 lasted for 10 seconds. Stage 1 of 0-1 seconds in the trial was the display of cues. Stage 2 of 1-6 seconds in the trial was the execution of the tasks according to the cues. Stage 3 of 6-10 seconds in the trial was the waiting stage for the next trial. The procedure of experiment I is shown in Figure 6. SSVEP session 1 consisted of 56 trials, indicated to the frequencies from 8 Hz to 14Hz. Motor imagery session 2 consisted of 50 trials, half of them were left-hand cues, the others were right-hand cues. In eyes-closed session 3, the trial consisted of two stages, executing cues in 0-5 seconds and waiting in 5-10 seconds. The cues were achieved by the sounds to prompt the subject to close eyes or open eyes. The users had 30 seconds break between the blocks to avoid fatigue in the off-line experiment. The off-line experiment I lasted for approximately 50 minutes with 5 minutes for resting between sessions.

Five subjects (2 males, 3 females), at the age of 20 to 24 (average age 23.1), participated in on-line experiment II. Five subjects continued to participate in on-line experiment II. They were familiar with the procedure of the experiment and the approach of system operation. The sketch of the experimental site and the position of targets are shown in Figure 7.

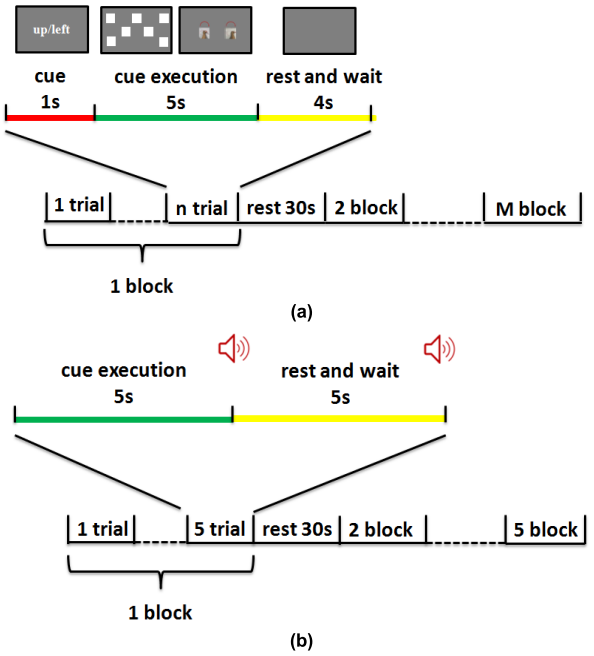

FIGURE 6. The procedure of the experiment I. (a) The procedure of session 1 and session 2. In session 1 (n = 8, M = 7), 56 trials (7 blocks) were involved. In session 2 (n = 5, M = 10), 50 trials (10 blocks) were involved. The cues were achieved by words in session 1 and image in session 2. (b) The procedure of session 3. 25 trials were involved. The cues were achieved by the sounds.

The on-line experiment II was conducted in the atrium of the laboratory building. The length of the atrium is 10m, while the width is 7.5m. The space outside the atrium was regarded as the wall. Four targets at different heights were placed in the atrium, with a length of 1m and width of 0.9m. The recording time in experiment II was set as 5 seconds, the control time of straight flight was set as 5 seconds, and the rotated flight was set as 7 seconds. The on-line experiment II was divided into three same sessions. The users controlled the quadcopter flight by using the stimulator interface. The visual feedback displayed the images captured by the camera of quadcopter and the position information of targets and quadcopter to help subjects make the right control command. In a session, subjects controlled the quadcopter to take off from the starting location, go through targets in turns, and land at the landing location. The quadcopter would land and take off again with the collision of the wall or the targets. The expert controlled the quadcopter to finish the same tasks with the android controller after 3 sessions of on-line experiment II. The experiement site and the subject are shown in Figure 8.

III. RESULTS

A. EXPERIMENT I

The alpha-band powers of EEG in the eyes-closed and eyes-open state were calculated with 10 subjects in off-line experiment I. The EEG in eyes-open state consisted of SSVEP and motor imagery. Furthermore, the percentage of alpha-band power in EEG signals with 10 subjects in two states and the classification thresholds were calculated by (3).

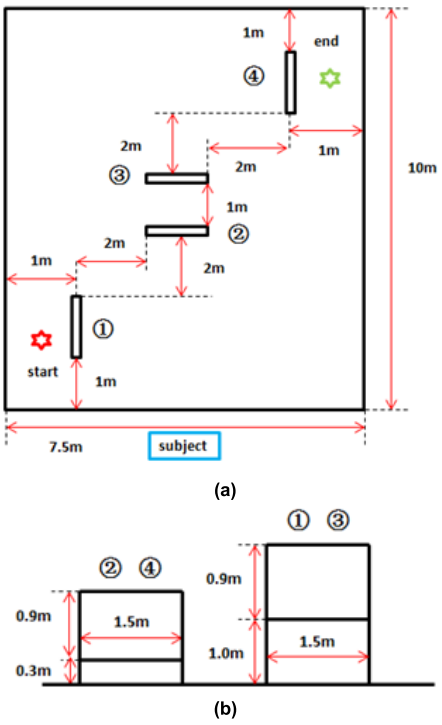

FIGURE 7. The sketch of site and targets in experiment II. (a) The site of experiment II. The length of the site is 7.5m and the width is 10m. Four square targets, indicated by the number, are placed for quadcopter to go through under the control of the users. The red and green star marks the starting position and the ending position of the quadcopter. (b) The schematic diagram of targets in experiment II. The target is 1.5m× 0.9m in size. The targets 1, 3 are 1m above the ground, and the targets 2, 4 are 0.3m above the ground.

The results are illustrated in Figure 9. It can be observed from the figure that the power percentages in eyes-closed state are obviously higher than those in eyes-open state, which reveals the feasibility of detection of two states by the percentage of alpha-band power in filtered-band power. Moreover, due to the alpha-band power differences in two states between 10 subjects, the selection of thresholds in detection are different between subjects.

The classification accuracies of SSVEP and motor imagery were compared between the different recorded data lengths and the different numbers of channels. The results with the one-way analysis of variance (ANOVA) are shown in Figure 10. Figure 10(a) shows the classification accuracy of SSVEP between the different recorded data lengths. There was a statistically significant difference between 5s and 2s, 3s, 4s recorded data lengths for the classification of SSVEP ($p < 0.05$). Figure 10(b) shows the classification accuracy of SSVEP between the different numbers of channels. The results illustrated a statistically significant difference between 1 channel, 3 channels and 9 channels selections for SSVEP classification ($p < 0.05$). The highest classification accuracy was 93.57±4.78% with 5s recorded data and 9 channels. Figure 10(c) and 10(d) show the classification accuracy of motor imagery between the different recorded data lengths and numbers of channels. The results showed that there was no statistically significant difference among the different recorded data lengths for motor imagery classification ($p > 0.05$). However, there was a statistically significant difference between 2 channels and 5 channels selections for the classification of motor imagery ($p < 0.05$). The highest classification accuracy was 71.76±10.53% with 5s recorded data length and 5channels selection.

Considering the consistency of the recording time in SSVEP and MI, the record time was set as 5s to ensure the high classification accuracy of the system. Besides that, the number of SSVEP channels was chosen 9 channels in the visual cortex. Though there was no statistically significant difference between 3 channels and 5 channels for motor imagery classification, the number of channels was chosen as 5 channels in the sensorimotor cortex due to the conservative consideration of the highest classification accuracy. Compared with the existing quadcopter control system [20], the classification accuracy of hybrid EEG was targeted as a priority in the parameter selection to optimize the control system.

The individual accuracy results of classification of eyes-closed state and eyes-open state, SSVEP classification and motor imagery classification for 10 subjects are illustrated in Table 3. The average classification accuracy of the eyes-closed state and eyes-open state was 90.86±6.43%. Meanwhile, the classification accuracy of the hybrid EEG in the off-line experiment was calculated by combined the classification accuracies of EEG in three states as following (11) and (12). η_{hybrid} indicated the classification accuracy of the hybrid EEG in the off-line experiment. η_{close} indicated the classification accuracy of the eyes-closed state. η_{open} indicated the classification accuracy of the eyes-open state. η_{SSVEP} indicated the classification accuracy of SSVEP. η_{MI} indicated the classification accuracy of motor imagery. K_{SSVEP} indicated the rate of SSVEP dataset in the eyes-open EEG. K_{MI} indicated the rate of motor imagery in the eyes-open EEG.

$$\eta_{open} = K_{SSVEP} \times \eta_{SSVEP} + K_{MI} \times \eta_{MI} \quad (11)$$

$$\eta_{hybird} = \eta_{close} \times \eta_{open} \quad (12)$$

B. EXPERIMENT II

The BCI control capacity of quadcopter flight was evaluated with 5 subjects in on-line experiment II. The capacity indicators are shown in Table 4, including classification accuracy in hybrid BCI, number of landing, command number rate and information rate. The average classification accuracy in hybrid BCI reached 87.09±2.82%, and the average information transfer rate was 0.857±0.085 bits/min. The results revealed the good detection performance of EEG-based commands and high robustness of the quadcopter control system based on hybrid BCI.

1) CLASSIFICATION ACCURACY IN HYBRID BCI

Classification accuracy in hybrid BCI indicates the performance of classifying EEG signals. Hybrid BCI was the combination of EEG in the eyes-closed state, SSVEP,

(a) (b)

FIGURE 8. The subject and experiment site in on-line expeiment II. (a) the subject gazed at the stimulator interface to control the quadcopter (b) the targets in experiment site.

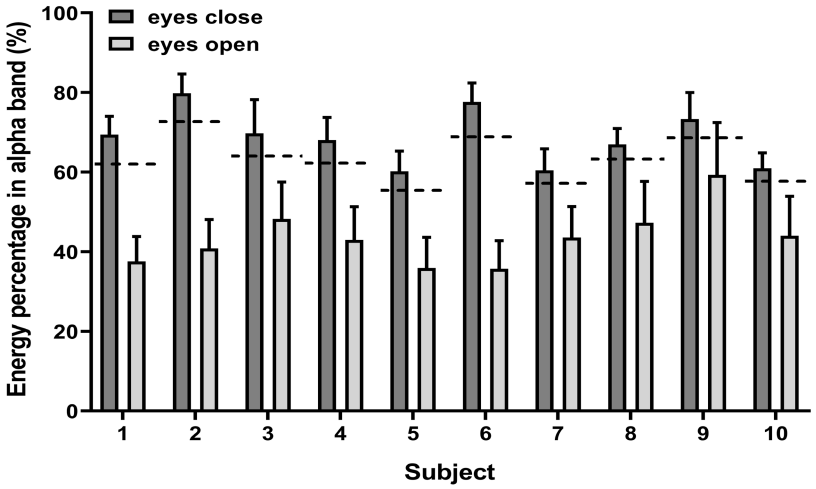

FIGURE 9. The percentage of the alpha-band power in the filtered-band power of the training data in eyes close and eyes open states, the EEG in eyes open state consisted of SSVEP and motor imagery EEG. The dotted line indicated the individual thresholds of the classifier in eyes close and eyes open classification.

and motor imagery. Classification accuracy in hybrid BCI was calculated by (13). In on-line experiment II, the classification accuracy in hybrid BCI was different due to the individual control strategy in quadcopter flight. The average classification accuracy in hybrid BCI with 5 subjects was 87.09±2.82%.

$$\text{Accuracy in classification} = \frac{\text{Number of correct EEG-based commands}}{\text{Number of EEG signals}} \quad (13)$$

2) NUMBER OF LANDING

Number of landing represented the number of quadcopter landing after a collision on wall or targets happened, due to the operational errors or the low precision of the control system. The average number of landing is 0.532±0.3 with 5 subjects in experiment II.

3) COMMAND NUMBER RATE

Command number rate is the ratio of the number of control commands based on the hybrid control system in one successful control trial to the number of control commands based on the android controller in one trial controlled by an expert, describing the classification capacity of quadcopter control system shown in equation (14). In experiment II, the expert finished the same control tasks by using the mobile app. The average control time was 3.4min, and the average number of the control command is 20. The average command number rate is 1.68±0.197. The results revealed the quadcopter control performance of hybrid BCI was lower than that of expert.

$$\text{Command number rate} = \frac{\text{Number of command use BCI}}{\text{Number of command use phone}} \quad (14)$$

4) INFORMATION TRANSFER RATE

Information transfer rate indicated the speed of information transfer, which was defined by Chen *et al.* [44], Shannon [45], and Li *et al.*[46]. Considering quadcopter flight and asynchronous BCI, information transfer rate was redefined as equation (15) by Lafleur *et al.* [10]. Displacement traveled to the target indicated the displacement between the starting position and ending position. Time to reach the target indicated the time of quadcopter flight from the starting position

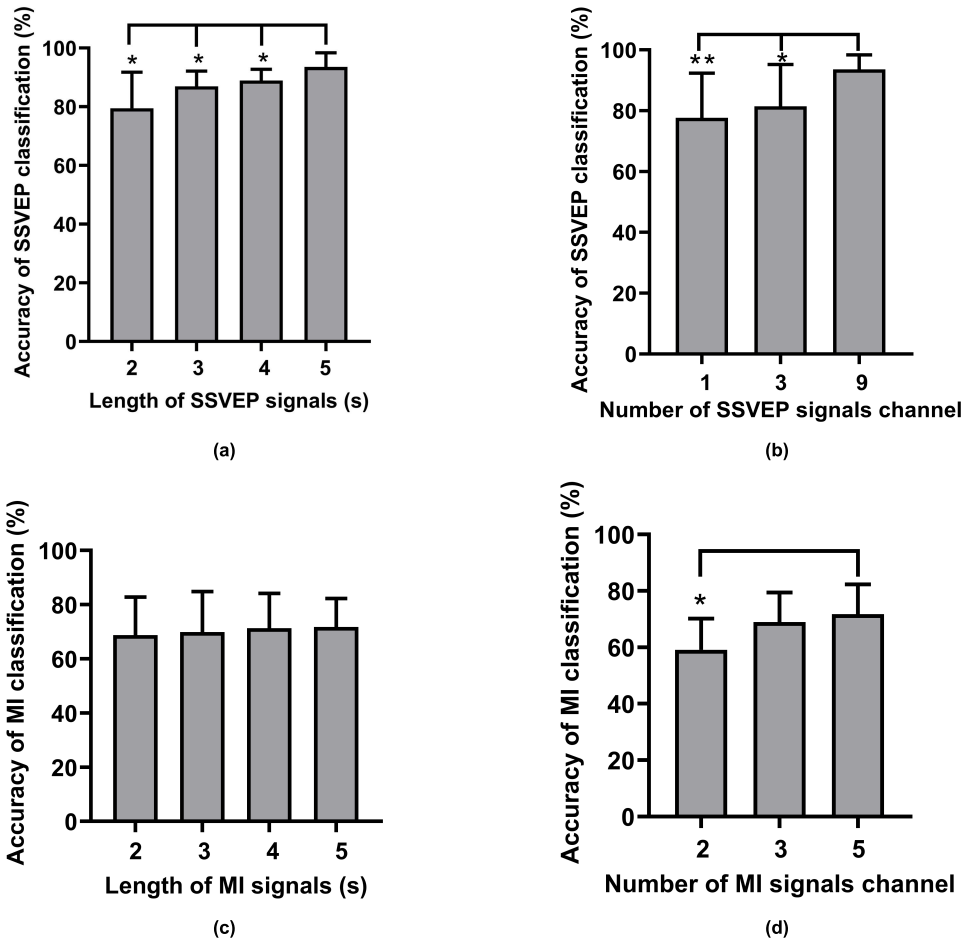

FIGURE 10. Diagrams showing the accuracy of SSVEP and motor imagery classification between the different recorded data length and the different number of channels (a) the recorded data length of SSVEP, which are 2s, 3s, 4s, 5s (b) the number of channels of SSVEP, which are 1(Oz), 3(O1, Oz, O2), 9(O1, Oz, O2, PO3, POz, PO4, P3, Pz, P4). (c) the recorded data length of motor imagery, which are 2s, 3s, 4s, 5s (d) the number of channels of motor imagery, which are 2(C3, C4), 3(Cz, C3, C4), 5(Cz, C1, C2, C3, C4).

to ending position. The average information transfer rate was 0.857±0.085 bit/min in experiment II.

$$\mathrm{ITR} = \frac{\log_2(\frac{\text{Displacement traveled to the target}}{\text{Length of the target}} + 1)}{\text{Time to reach the target}} \tag{15}$$

IV. DISCUSSION

In the study, a quadcopter control system was accomplished by taking advantage of hybrid BCI technology. The hybrid BCI avoided the limited number of commands in MI-based BCI and the weak correlation between users' intention and the control command in SSVEP-based BCI, which was regarded as the combination of SSVEP-based BCI and MI-based BCI. Moreover, the off-line optimization and the human-machine interaction enhancement improved the practicability and operability in real-time use. Compared with the existing quadcopter control system [5], [20], the proposed system has three unique features. Firstly, the proposed system has the advantage of multidirectional control in quadcopter flight by the hybrid BCI. The degrees of freedoms contain six directions in 3D space which demonstrates the feasibility of the complex control in the physical world. Secondly, the proposed system is optimized by the off-line experiment results. The high classification accuracy is targeted as a priority in the optimal parameter selections, which may reduce the speed of the control system. However, the results in the on-line experiment revealed the significance in the optimization. The proposed control system finished the more complex route task with a higher success rate than the other quadcopter control system by hybrid BCI [20]. Thirdly, the proposed system enhances the human-machine interaction in designs, including choosing EEG in the eyes-closed state as the switch signal between SSVEP and motor imagery, displaying the feedback information for users and providing the LCD-cued SSVEP and MI, which improves the operability of the control system.

The control precision is a common problem in quadcopter control. Due to the draining battery, the movement displacement and yaw angle with the same command often slightly changed during the quadcopter flight, which led the difficulties for users to control quadcopter to reach the targets. Moreover, the quadcopter was hard to keep the stable state during the hovering stage, which led to the position error

TABLE 3. Individual classification of EEG in eyes close state, SSVEP and motor imagery EEG in experiment I.

Subject	Accuracy in EEG signals classification			
	Eyes close and open	SSVEP	MI	Hybrid signals
Subject1	95.96%	96.43%	79.20%	85.20%
Subject2	96.23%	98.21%	57.20%	76.37%
Subject3	85.34%	87.50%	61.60%	64.62%
Subject4	95.69%	94.64%	86.40%	87.30%
Subject5	92.24%	94.64%	76.00%	79.63%
Subject6	96.55%	89.26%	65.20%	75.66%
Subject7	94.83%	89.26%	60.80%	72.34%
Subject8	90.52%	87.50%	86.80%	79.30%
Subject9	79.31%	98.21%	74.00%	69.23%
Subject10	81.90%	100%	70.40%	70.88%
Mean	90.86%	93.57%	71.52%	76.05%
Standard Error	6.43%	4.78%	10.53%	7.08%

TABLE 4. The performance of 5 subjects in on-line experiment II.

n	Trial	Classification accuracy		Number of landing		Command number rate		Information transfer rate	
		Individual	Mean	Individual	Mean	Individual	Mean	Individual	Mean
S2	1	89.29%	85.32%	1	0.33	1.4	1.55	0.9447	0.8794
	2	86.67%		0		1.5		0.9088	
	3	80.00%		0		1.75		0.7847	
S4	1	87.88%	85.72%	1	1	1.65	1.97	0.8497	0.7241
	2	82.93%		2		2.05		0.6871	
	3	86.36%		0		2.2		0.6354	
S8	1	90.90%	92.07%	0	0.33	1.65	1.47	0.8599	0.9538
	2	96.43%		1		1.4		0.9972	
	3	88.89%		0		1.35		1.0042	
S9	1	93.10%	85.79%	1	0.67	1.45	1.77	0.9769	0.8156
	2	85.71%		0		1.75		0.8113	
	3	78.57%		1		2.1		0.6587	
S10	1	75.00%	86.55%	0	0.33	1.8	1.63	0.7479	0.86
	2	96.43%		1		1.4		0.9972	
	3	88.23%		0		1.7		0.8348	
Group mean	/	/	87.09±2.82%	/	0.532±0.3	/	1.68±0.197	/	0.8566± 0.0847

in physical space. All the above problems in quadcopter control caused the differences between the simple machine control and the practical quadcopter control [10], [47]. Two novel commands were proposed to adjust the quadcopter displacement by moving left and right to reduce the quadcopter position errors in hovering. The results in this study revealed the effectiveness of the proposed scheme in the position error reduction of the practical quadcopter control.

In the proposed system, the eyes-closed state was chosen as the switch signal of SSVEP and motor imagery. In fact, some classification algorithms had been tried by using the EEG signals from the off-line experiment [9], [25], [26]. The results are shown in Table 5. The detections of the eyes-closed state and the eyes-open state were achieved by the alpha-band power percentage, due to the spontaneous activity of the mind was more active in the eyes-open state [27]. The threshold of the detection was selected as the weighted sum of the alpha-band power in the eyes-closed state and the eyes-open state as formula (3). The rate of weight and the detection results are shown in Figure 11. It can be observed from the figure that the optimal result corresponds to the weight rate of 8:2 with $power_{close}$ and $power_{open}$. The alpha-band power gradually rose due to the fatigue of subjects in the eyes-open state during the operation process. As shown in Figure 9, the variance of the alpha-band power in the eyes-open state is higher than the eyes-closed state, which illustrated the fluctuation of the alpha-band power in the eyes-open state. In the off-line experiment I, the alpha-band power percentage of some datasets were higher than $(power_{close}+power_{open})/2$, which caused the detection result of 8:2 was better than 5:5.

The BCI control capacity of quadcopter flight was evaluated in the on-line experiment II. The main capacity indicators were classification accuracy in hybrid BCI and information transfer rate. The classification accuracy of the hybrid EEG in the off-line experiment I was 76.05±7.08%, while the classification accuracy in the hybrid BCI in the on-line experiment was 87.09±2.82%. The classification results both in off-line experiment I and on-line experiment II

TABLE 5. The classification accuracy of swithcing between ssvep and motor imagery.

Paper	J. Li et al. [9]	K. L. Wei et al. [23]	Z. Cao et al. [33]	Our study
Method	Features-SVM	Correlations-threshold	STFT-ERS	Eyes-closed state
Accuracy(%)	74.43±8.31	65.09±12.59	62.76±12.57	90.86±6.43

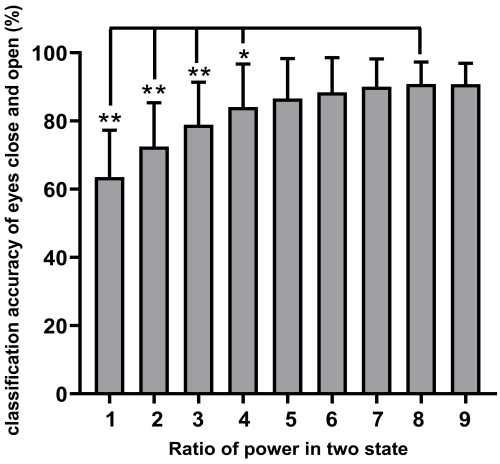

FIGURE 11. The detection results of eyes close and open with the different thresholds selection. The thresholds were selected by variable of selected weights in equation (21). The ratio of power percentage in eyes close and open state, regarded as the selected weight, were shown above. 1 indicated the ratio of 1:9, 2 indicated the ratio of 2:8, 3 indicated the ratio of 3:7, 4 indicated the ratio of 4:6, 5 indicated the ratio of 5:5, 6 indicated the ratio of 6:4, 7 indicated the ratio of 7:3, 8 indicated the ratio of 8:2, 9 indicated the ratio of 9:1.

indicated the classification capacity of the hybrid BCI. The difference between classification accuracies in off-line experiment I and on-line experiment II can be explained by the following points. On one hand, the different control strategies in on-line experiment II caused the EEG data imbalanced distribution, which had an impact on the classification accuracy [48]. In off-line experiment I, the results revealed that the accuracy classification of SSVEP was higher than motor imagery. Compared with the amount of dataset recorded in off-line experiment I, the percentage of SSVEP in the amount of total dataset was higher in on-line experiment II. Considering the accuracy of SSVEP is higher than motor imagery, it can be used to explain that the total classification accuracy in experiment II is higher than in experiment I. On the other hand, all 5 subjects in experiment II had participated in experiment I. The familiarity of quadcopter control system was also an explanation for the improvement of classification accuracy. The average information transfer rate was only 0.857±0.085bit/min. After the construction of the control system and design of the on-line experiment, the length of targets and displacement travel to the target were set as a constant. According to formula (15), the improvement of information transfer rate would be achieved by reducing the control time in the same control tasks. On one hand, the recording time in experiment II was set as 5 seconds, the control time of straight flight was set as 5 seconds, and the rotated flight was set as 7 seconds. The too-long command time of the quadcopter control system was the key reason for the low information transfer rate. On the other hand, the unnecessary commands caused by the low control precision of the control system increased the control time of the system, which also led to the low information transfer rate. Low information transfer rate is the primary defect of the proposed system, we will focus on it in future work.

In future work, the improvement of information transfer rate as the main optimization target of the proposed system should be focused on. The results in experiment II revealed that reduction of the control time in quadcopter flight with the same tasks is an approach to improving the information transfer rate in the control system. Firstly, the EEG recording time and training time would be reduced by the improvement of the feature extraction and classification algorithm under the premise of the high accuracy of the control system [49]–[52]. Secondly, the framework strategy of the control system and the procedure of the quadcopter control could be simplified to reduce the unnecessary commands in the quadcopter control. On one hand, the adjustment commands caused by the shifts during the hovering stage should be reduced by improving the precision of the control system. On the other hand, an effective algorithm classifying between SSVEP and motor imagery EEG would be proposed to reduce the control time of the eyes-closed state. Moreover, the detection of idle time should be considered into the control system to establish an asynchronous BCI to improve the performance of the quadcopter control system [53].

V. CONCLUSION

In this study, a quadcopter control system using a hybrid BCI based on off-line optimization and enhanced human-machine interaction was constructed to control the quadcopter flight in 3D space. The proposed system controlled the quadcopter with eight EEG-based control commands, including six commands based on SSVEP controlling the straight flight and two commands based on motor imagery controlling the rotated flight, which met the demands of multidirectional control in human daily life. Meanwhile, a scheme based on the detection of eyes closed and open to classify SSVEP and motor imagery was presented, which was able to accomplish the high accuracy and high robustness of the control system. Moreover, the parameters of the control system were optimized and the human-machine interaction was enhanced to improve practicability in real-time use. The proposed control system establishes a framework for the implementation of the quadcopter control based on hybrid BCI.

REFERENCES

[1] S. Gao, Y. Wang, X. Gao, and B. Hong, "Visual and auditory brain-computer interfaces," *IEEE Trans. Biomed. Eng.*, vol. 61, no. 5, pp. 1436–1447, May 2014.
[2] X. Chen, B. Zhao, Y. Wang, S. Xu, and X. Gao, "Control of a 7-DOF robotic arm system with an SSVEP-based BCI," *Int. J. neural Syst.*, vol. 28, no. 8, 2018, Art. no. 1850018.
[3] E. Yin, Z. Zhou, J. Jiang, Y. Yu, and D. Hu, "A dynamically optimized SSVEP Brain–Computer interface (BCI) speller," *IEEE Trans. Biomed. Eng.*, vol. 62, no. 6, pp. 1447–1456, Jun. 2015.

[4] Q. Zhao, L. Zhang, and A. Cichocki, "EEG-based asynchronous BCI control of a car in 3D virtual reality environments," *Chin. Sci. Bull.*, vol. 54, no. 1, pp. 78–87, Jan. 2009.

[5] A. Nourmohammadi, M. Jafari, and T. O. Zander, "A survey on unmanned aerial vehicle remote control using brain–computer interface," *IEEE Trans. Human-Mach. Syst.*, vol. 48, no. 4, pp. 337–348, Aug. 2018.

[6] L. Meriño, "Asynchronous control of unmanned aerial vehicles using a steady-state visual evoked potential-based brain computer interface," *Brain-Comput. Inter.*, vol. 4, nos. 1–2, pp. 122–135, 2017.

[7] M. Wang, R. Li, R. Zhang, G. Li, and D. Zhang, "A wearable SSVEP-based BCI system for quadcopter control using head-mounted device," *IEEE Access*, vol. 6, pp. 26789–26798, 2018.

[8] Y. Wang and T.-P. Jung, "Visual stimulus design for high-rate SSVEP BCI," *Electron. Lett.*, vol. 46, no. 15, pp. 1057–1058, 2010.

[9] J. Li, H. Ji, L. Cao, D. Zang, R. Gu, B. Xia, and Q. Wu, "Evaluation and application of a hybrid brain computer interface for real wheelchair parallel control with multi-degree of freedom," *Int. J. Neural Syst.*, vol. 24, no. 4, 2014, Art. no. 1450014.

[10] K. LaFleur, K. Cassady, A. Doud, K. Shades, E. Rogin, and B. He, "Quadcopter control in three-dimensional space using a noninvasive motor imagery-based brain-computer interface," *J. Neural Eng.*, vol. 10, no. 4, Aug. 2013, Art. no. 046003.

[11] T. Shi, H. Wang, and C. Zhang, "Brain computer interface system based on indoor semi-autonomous navigation and motor imagery for Unmanned Aerial Vehicle control," *Expert Syst. Appl.*, vol. 42, no. 9, pp. 4196–4206, Jun. 2015.

[12] M. Kaya, M. K. Binli, E. Ozbay, H. Yanar, and Y. Mishchenko, "A large electroencephalographic motor imagery dataset for electroencephalographic brain computer interfaces," *Sci. Data*, vol. 5, Oct. 2018, Art. no. 180211.

[13] S. Zhang, S. Wang, D. Zheng, K. Zhu, and M. Dai, "A novel pattern with high-level commands for encoding motor imagery-based brain computer interface," *Pattern Recognit. Lett.*, vol. 125, pp. 28–34, Jul. 2019.

[14] Z. Wang, Y. Yu, M. Xu, Y. Liu, E. Yin, and Z. Zhou, "Towards a hybrid BCI gaming paradigm based on motor imagery and SSVEP," *Int. J. Hum.-Comput. Interact.*, vol. 35, no. 3, pp. 197–205, 2019.

[15] B. H. Kim, M. Kim, and S. Jo, "Quadcopter flight control using a low-cost hybrid interface with EEG-based classification and eye tracking," *Comput. Biol. Med.*, vol. 51, pp. 82–92, Aug. 2014.

[16] M. J. Khan and K.-S. Hong, "Hybrid EEG-fNIRS-based eight-command decoding for BCI: Application to quadcopter control," *Frontiers Neurorobot.*, vol. 11, p. 6, Feb. 2017.

[17] G. Wang, Z. Liu, Y. Feng, J. Li, H. Dong, D. Wang, J. Li, N. Yan, T. Liu, and X. Yan, "Monitoring the depth of anesthesia through the use of cerebral hemodynamic measurements based on sample entropy algorithm," *IEEE Trans. Biomed. Eng.*, to be published.

[18] X. Duan, S. Xie, X. Xie, Y. Meng, and Z. Xu, "Quadcopter flight control using a non-invasive multi-modal brain computer interface," (in English), *Frontiers Neurorobot., Original Res.*, vol. 13, p. 23, May 2019.

[19] F. Duan, D. Lin, W. Li, and Z. Zhang, "Design of a multimodal EEG-based hybrid BCI system with visual servo module," *IEEE Trans. Auton. Mental Develop.*, vol. 7, no. 4, pp. 332–341, Dec. 2015.

[20] X. Chen, Y. Wang, M. Nakanishi, X. Gao, T.-P. Jung, and S. Gao, "High-speed spelling with a noninvasive brain-computer interface," *Proc. Nat. Acad. Sci. USA*, vol. 112, no. 44, pp. E6058–E6067, 2015.

[21] D. H. Brainard, "The psychophysics toolbox," *Spatial Vis.*, vol. 10, no. 4, pp. 433–436, 1997.

[22] G. Wang and D. Ren, "Effect of brain-to-skull conductivity ratio on EEG source localization accuracy," *BioMed Res. Int.*, vol. 2013, Mar. 2013, Art. no. 459346.

[23] L.-W. Ko, S. S. K. Ranga, O. Komarov, and C.-C. Chen, "Development of single-channel hybrid BCI system using motor imagery and SSVEP," *J. Healthcare Eng.*, vol. 2017, Jun. 2017, Art. no. 3789386.

[24] O. Dehzangi, Y. Zou, and R. Jafari, "Simultaneous classification of motor imagery and SSVEP EEG signals," in *Proc. 6th Int. IEEE/EMBS Conf. Neural Eng. (NER)*, Nov. 2013, pp. 1303–1306.

[25] Z. Cao, C.-H. Chuang, J.-K. King, and C.-T. Lin, "Multi-channel EEG recordings during a sustained-attention driving task," *Sci. Data*, vol. 6, p. 19, Apr. 2019.

[26] W. Shi, Y. Li, Z. Liu, J. Li, and G. Wang, "Non-canonical microstate becomes salient in high density EEG during propofol-induced altered states of consciousness," *Int. J. Neural Syst.*, to be published.

[27] L. Li, L. Xiao, and L. Chen, "Differences of EEG between eyes-open and eyes-closed states based on autoregressive method," *J. Electron. Sci. Technol.*, vol. 7, no. 2, pp. 175–179, 2009.

[28] J. Sherwood and R. Derakhshani, "On classifiability of wavelet features for EEG-based brain-computer interfaces," in *Proc. Int. Joint Conf. Neural Netw.*, Jun. 2009, pp. 2895–2902.

[29] Y. Zhang, G. Wang, C. Teng, Z. Sun, and J. Wang, "The analysis of hand movement distinction based on relative frequency band energy method," *BioMed Res. Int.*, vol. 2014, Sep. 2014, Art. no. 781769.

[30] C.-S. Hsieh and C.-C. Tai, "Subjective mood estimation using power energy of EEG frequency band," in *Proc. Int. Symp. Next-Gener. Electron.*, Feb. 2013, pp. 517–520.

[31] G. Wang, C. Teng, K. Li, Z. Zhang, and X. Yan, "The removal of EOG artifacts from EEG signals using independent component analysis and multivariate empirical mode decomposition," *IEEE J. Biomed. Health Inform.*, vol. 20, no. 5, pp. 1301–1308, Sep. 2016.

[32] Z. Cao, W. Ding, Y.-K. Wang, F. K. Hussain, A. Al-Jumaily, and C.-T. Lin, "Effects of repetitive SSVEPs on EEG complexity using multiscale inherent fuzzy entropy," *Neurocomputing*, to be published.

[33] Z. Cao, C.-T. Lin, K.-L. Lai, L.-W. Ko, J.-T. King, K.-K. Liao, J.-L. Fuh, and S.-J. Wang, "Extraction of SSVEPs-based inherent fuzzy entropy using a wearable headband EEG in migraine patients," *IEEE Trans. Fuzzy Syst.*, to be published.

[34] G. Bin, X. Gao, Z. Yan, B. Hong, and S. Gao, "An online multi-channel SSVEP-based brain-computer interface using a canonical correlation analysis method," *J. Neural Eng.*, vol. 6, no. 4, 2009, Art. no. 046002.

[35] S.-L. Wu, C.-W. Wu, N. R. Pal, C.-Y. Chen, S.-A. Chen, and C.-T. Lin, "Common spatial pattern and linear discriminant analysis for motor imagery classification," in *Proc. IEEE Symp. Comput. Intell., Cogn. Algorithms, Mind,Brain (CCMB)*, Apr. 2013, pp. 146–151.

[36] M. Cheng, X. Gao, S. Gao, and D. Xu, "Design and implementation of a brain-computer interface with high transfer rates," *IEEE Trans. Biomed. Eng.*, vol. 49, no. 10, pp. 1181–1186, Oct. 2002.

[37] C. E. Shannon, "A mathematical theory of communication," *Bell Syst. Tech. J.*, vol. 27, no. 3, pp. 379–423, Jul./Oct. 1948.

[38] A. Doud, K. LaFleur, K. Shades, E. Rogin, K. Cassady, and B. He, "Noninvasive brain-computer interface control of a quadcopter flying robot in 3D space using sensorimotor rhythms," in *Proc. World Congr. Medical Phys. Biomed. Eng.*, 2012.

[39] H. He and E. A. Garcia, "Learning from imbalanced data," *IEEE Trans. Knowl. Data Eng.*, vol. 21, no. 9, pp. 1263–1284, Sep. 2009.

[40] X. Chen, Z. Chen, S. Gao, and X. Gao, "A high-ITR SSVEP-based BCI speller," *Brain-Comput. Interfaces*, vol. 1, nos. 3–4, pp. 181–191, 2014.

[41] Z. Zhang, F. Duan, J. Solé-Casals, J. Dinarès-Ferran, A. Cichocki, Z. Yang, and Z. Sun, "A novel deep learning approach with data augmentation to classify motor imagery signals," *IEEE Access*, vol. 7, pp. 15945–15954, 2019.

[42] D. Zhang, Y. Wang, X. Gao, B. Hong, and S. Gao, "An algorithm for idle-state detection in motor-imagery-based brain-computer interface," *Comput. Intell. Neurosci.*, vol. 2007, p. 5, Jan. 2007.

NONG YAN received the B.S. degree in biomedical engineering from Xi'an Jiaotong University, Xi'an, China, in 2017, where he is currently pursuing the M.S. degree in biomedical engineering. His research interests include brain–computer interface, biomedical signal processing, and machine learning.

CHANG WANG is currently pursuing the B.S. degree in biomedical engineering with Xi'an Jiaotong University, Xi'an, China. Her research interests include brain–computer interface and ultrasound imaging.

YI TAO received the B.S. degree in biomedical engineering from Nanchang University, Nanchang, China. She is currently pursuing the M.S. degree in biomedical engineering with Xi'an Jiaotong University, Xi'an, China. Her research interests include brain–computer interface and signal processing.

JINMING LI received the B.S. degree in biomedical engineering from Xi'an Jiaotong University, Xi'an, China, in 2019. He is currently pursuing the M.S. degree in biomedical engineering with Shanghai Jiaotong University, Shanghai, China. His research interests include brain–computer interface, biomedical imaging, and deep learning.

KEXU ZHANG is currently pursuing the B.S. degree in biomedical engineering with Xi'an Jiaotong University, Xi'an, China. His research interests include brain–computer interface and EEG signals processing.

TING CHEN is currently pursuing the B.S. degree in biomedical engineering with Xi'an Jiaotong University, Xi'an, China. Her research interests mainly focus on biomedical signal processing and rehabilitation engineering.

ZIWEN YUAN received the M.S. degree in neurology from Forth Military Medical University, Xi'an, China. His research interests mainly focus on neurology and neurological rehabilitation.

XIANGGUO YAN received the B.S. degree in industrial automation from the Zhengzhou University of Light Industry, Zhengzhou, China, in 1983, the M.S. degree in automatic control and the Ph.D. degree in biomedical engineering from Xi'an Jiaotong University, Xi'an, China, in 1990 and 1995, respectively.

From 1996 to 1998, he was a Visiting Scientist with the Juelich Research Center, Germany. He is currently a Professor with the School of Life Science and Technology, Xi'an Jiaotong University. His main research interests are biomedical signal and image processing, and the development of medical instrumentation.

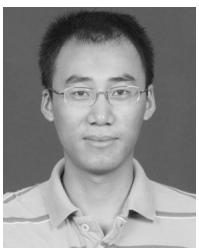

GANG WANG (M'12) received the Ph.D. degree in biomedical engineering from Shanghai Jiao Tong University, Shanghai, China, in 2008.

He was a Postdoctoral Associate with the Department of Biomedical Engineering, University of Minnesota, Twin Cities. Since 2016, he has been with the faculty of Xi'an Jiaotong University as an Associate Professor with the School of Life Science and Technology and the Institute of Biomedical Engineering. He has authored more than 40 international journal articles and holds a number of patents and copyrights. His research interests include biomedical functional neuroimaging, biomedical signal processing, neural engineering, and bioelectromagnetism.